Measurements of the electron swarm parameters of R1225ye(Z) (C3HF5) and its mixtures with N2 and CO2

Author(s):
Pachin, Juriy; Hösl, Andreas; Franck, Christian

Publication date:
2019-04-03

Permanent link:
https://doi.org/10.3929/ethz-b-000303118

Originally published in:
Journal of Physics D 52(23), https://doi.org/10.1088/1361-6463/ab0f5c

Measurements of the Electron Swarm Parameters of R1225ye(Z) (C_3HF_5) and its Mixtures with N_2 and CO_2

Juriy Pachin and Christian M. Franck

ETH Zurich, High Voltage Laboratory, Physikstr. 3, 8092 Zurich, Switzerland

E-mail: jpachin@ethz.ch

Abstract. The electron swarm parameters of R1225ye(Z) (cis-1, 2, 3, 3, 3-pentafluoroprop-1-ene) and its mixtures with the buffer gases N_2 and CO_2 from 1% to 50% are experimentally investigated using a pulsed Townsend experiment. The analysis of the electron avalanche displacement current yields the effective ionization rate coefficient, the electron drift velocity and the longitudinal electron diffusion coefficient. To assess the potential of the gas as an insulating medium for medium or high voltage applications, the density-reduced critical electric field $(E/N)_{\mathrm{crit}}$ is obtained. In pure R1225ye(Z), $(E/N)_{\mathrm{crit}}$ increases with increasing pressure from around 280 Td at 2 kPa to 300 Td at 14 kPa. Mixtures of R1225ye(Z) with N_2 and CO_2 show almost no synergy. Finally a comparison to HFO1234ze(E) and l-C_3F_6 is given.

1. Introduction

The computational screening method of Rabie et al. [1, 2] for new high-voltage insulation gases with low global warming potential (GWP), showed R1225ye(Z) as one of the promising candidates. R1225ye(Z) is commercially available and has a molecular structure similar to the previously investigated HFO1234ze(E) [3, 4] and l-C_3F_6 [5]. Due to these reasons, pure R1225ye(Z) and its mixtures with buffer gases N_2 and CO_2 were chosen to be investigated in a pulsed Townsend experiment, to obtain their electron swarm parameters and determine $(E/N)_{\mathrm{crit}}$. This allows, in combination with the knowledge of the liquefaction temperature, the first estimation of the insulation performance.

In high-voltage equipment, SF_6 is predominately used as a gaseous insulation medium. The main advantages are its high $(E/N)_{\mathrm{crit}}$, chemical stability, zero toxicity, and in particular, a low liquefaction temperature. However, the main disadvantage of SF_6 is its GWP - being 23 500 times that of CO_2 on a 100-year time horizon [6] - which therefore requires a replacement by an environment-friendly substance.

This work is structured as follows: Section 2 describes the properties of R1225ye(Z), the pulsed Townsend setup, and the method for analyzing measurements. Section 3 presents the obtained electron swarm parameters of pure R1225ye(Z) and its mixtures with N_2 and CO_2 - for different mixing ratios and pressures. The swarm parameters are: the effective ionization rate coefficient k_{eff}, electron drift velocity w_{e}, and electron longitudinal diffusion coefficient ND_{L}. In Section 4, the three-body electron attachment properties of R1225ye(Z) are discussed, the $(E/N)_{\mathrm{crit}}$ of different mixtures with N_2 and CO_2 are summarized, and a comparison with HFO1234ze(E) and l-C_3F_6 is shown.

2. Methods

2.1. R1225ye(Z)

R1225ye(Z) is also known as HFO1225ye(Z), (Z)-HFC-1225ye, cis-1,2,3,3,3-pentafluoroprop-1-ene, (Z)-1,2,3,3,3-Pentafluoropropene, CF3CF=CHF(Z) or C_3HF_5 with the CAS number 5528-43-8. The molecular structure of R1225ye(Z) is illustrated in figure 5(a). It was considered as a medical propellant [7], or by the automotive industry as a possible component of an alternative refrigerant blend with low GWP [8]. R1225ye(Z) has a GWP $<$ 1 with an atmospheric lifetime of 8.5 days [6]. The acute toxicity LC_{50} for 4 h inhalation by rats is above 50 000 ppm. Rat inhalation studies for 28 days show toxicological effects at 10 000, 25 000, and 50 000 ppm concentrations [7]. R1225ye(Z) is claimed to be non-flammable and chemically stable [8–10]. The molecular mass is 132.03 g/mol. The normal boiling point is 253.6 K, the vapor pressure at 293.15 K is 0.436 MPa, the ideal gas specific heat at constant pressure and 300 K is 101.9 kJ·(kmol·K)$^{-1}$ [8]. The normal boiling point of R1225ye(Z) is around 44 K above the boiling point of SF_6. To avoid liquefaction by similar operating conditions to SF_6 equipment, R1225ye(Z) has to be used in mixture with buffer gases. The $(E/N)_{\mathrm{crit}}$ of these gas mixtures must be also investigated, as it can exceed the linear combination of $(E/N)_{\mathrm{crit}}$ of the individual gas components weighted by their mole fraction. This beneficial effect for the insulation application is called synergy [11, 12]. The maximal mole-fractions of R1225ye(Z) in N_2 and CO_2, for technically relevant pressures and temperatures are listed in table 1.

The purity of the R1225ye(Z) sample was 97%, the impurity consisting mainly of the R1225ye(E)-isomer [13] . The purity of N_2 was 6.0, and the purity of CO_2

Table 1. Maximal mole-fraction of R1225ye(Z) in mixture with N_2 and CO_2, assuming ideal gases, filling at 293 K, considering different minimal operating temperatures according to the requirements of IEC 62271-1 [14].

minimal operating temperature (K)	filling pressure at 293 K	maximal mole fraction of R1225ye(Z) (%) in N_2	in CO_2
(in- and outdoor) 248	140	67	65
	600	16	11
(indoor) 258	140	99	99
	600	23	18
(outdoor) 263	140	100	100
	600	23	19
(indoor) 268	140	100	100
	600	33	29

was 4.8. The gases were mixed by partial pressures under the assumption of validity of the ideal gas law.

2.2. Experimental Setup

The measurements of electron swarm parameters were performed in the pulsed Townsend (PT) setup, described in detail by Dahl et al. [15]. A schematic of the PT-experiment is shown in Figure 1. For the investigation, the gas was filled into a pressure vessel containing two electrodes with a Rogowski profile and an adjustable gap distance d. Before filling the gases, the vessel was evacuated to a pressure below 1 Pa. A negative voltage U in the range from -0.2 kV up to -40 kV has been applied to the back-illuminated photocathode, while the anode was grounded. A short UV-laser pulse, with a wavelength of 266 nm, a duration of 1.5 ns FWHM and a repetition rate of 20 Hz, releases approximately 10^7 electrons from the cathode. Due to the applied homogeneous electric field E, the released electrons drift in a swarm towards the anode and collide with sample gas molecules in the vessel. The collisions may lead to ionization and attachment events. The ionization forms positive ions and simultaneously releases new free electrons. The attachment forms negative ions by capturing free electrons. Consequently, the number of electrons in the swarm increases or decreases.
All measurements were performed at a monitored room temperature. Each E/N value was measured at several pressure levels and at four discrete electrode distances, namely 19 mm, 17 mm, 15 mm, and 13 mm for each pressure level.

2.3. Measurement Analysis

The displacement current resulting from the electron and ion drift in the gap was measured at the anode, thus allowing extraction of the electron swarm parameters with the method described by Chachereau et al. [3]. Examples of electron current waveforms are

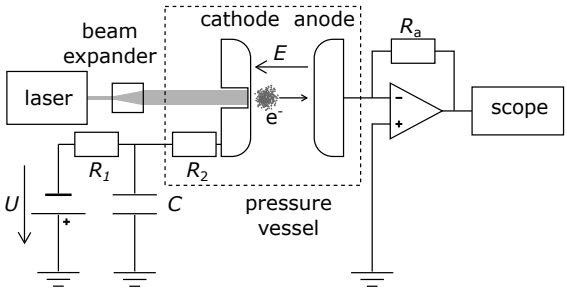

Figure 1. Schematic of the pulsed Townsend experiment ($R_1 = 180\ \Omega$, $R_2 = 100\ \Omega$, $C = 2$ nF) [4]

.

shown in figure 2. The electron swarm is modeled with a Gaussian spatial distribution along the propagation axis. The corresponding electron current I_e can be expressed for $t \geqslant 0$ as equation (1) [3, 15]

$$I_e(t) = \frac{I_0}{2} \exp\left(k_{\text{eff}} N t\right) \left(1 - \text{erf}\left(\frac{t - t_e}{\sqrt{2\tau_D t}}\right)\right), \qquad (1)$$

where I_0 is the electron current at time $t = 0$, k_{eff} the effective ionization rate coefficient, t_e the electron drift time in the gap, and τ_D the characteristic time for longitudinal electron diffusion. The canonical error function 'erf' describes the electron swarm absorption at the anode. It is assumed that the laser pulse releases the electrons in an initial distribution of a Dirac delta function. By fitting equation (1), the swarm parameters: effective ionization rate coefficient k_{eff}, bulk electron drift velocity $w_e = d/t_e$, and electron longitudinal diffusion coefficient $ND_L = w_e^2 \tau_D N/2$ are obtained. They depend on the density-reduced electric field E/N with the unit Townsend ($1\ \text{Td} = 10^{-21}\ \text{Vm}^2$). The gas number density $N = p/(k_B \cdot T)$ depends on the gas pressure p and the temperature T, k_B is the Boltzmann constant.
The main quantity to characterize the dielectric performance of an insulating gas in a PT-experiment is the density-reduced critical electric field $(E/N)_{\text{crit}}$. It corresponds to the breakdown field in a homogeneous field configuration for large electrode gaps and high pressures. The condition of $E/N = (E/N)_{\text{crit}}$ is fulfilled if the number of electrons in the swarm stays constant, i.e. $k_{\text{eff}} = 0$. If electron attachment is dominant, the number of electrons in the swarm decreases, consequently $k_{\text{eff}} < 0$ and $E/N < (E/N)_{\text{crit}}$. If ionization is dominant, the number of electrons in the swarm increases, i.e. $k_{\text{eff}} > 0$ and $E/N > (E/N)_{\text{crit}}$. These relations are illustrated by the example current traces in figure 2.

3. Results

The swarm parameters were obtained for the widest possible E/N range. Outside this range the signal is too low for the evaluation. This was the case for strong electron attachment and high pressures. For strong electron attachment and a sufficiently strong signal, the current decreased to zero before the swarm could reach the anode. Consequently, it was not possible to determine w_e and ND_L. For higher pressures the bandwidth of the amplifier was not high enough to obtain ND_L. In this work, the most relevant data are presented. The whole set of measurement data is available on the LXcat website, database ETHZ [16, 17].

3.1. R1225ye(Z) at different pressures

Pure R1225ye(Z) was measured in the pressure range from 2 kPa to 14 kPa - in 2 kPa steps. Sample electron currents are shown in figure 2. In figure 2(a), the pressure was kept constant at 2 kPa while the E/N value was changed by changing the cathode voltage. $(E/N)_{crit}$ is around 280 Td. Vice-versa in figure 2(b), the pressure levels were varied, while the E/N value was kept constant at 286 Td. With an increasing pressure, k_{eff} changes from negative to positive values. Figure 3(a) shows k_{eff}, as a function of E/N for different pressures in pure R1225ye(Z). k_{eff} decreases with increasing pressure as already shown in figure 2(b). Consequently, $(E/N)_{crit}$ increases.

3.2. R1225ye(Z)/N_2 mixtures

Figure 3 shows k_{eff}, w_e, and ND_L as functions of E/N for R1225ye(Z)/N_2 mixtures, with a R1225ye(Z) mole fraction from 5% to 50%. The pressure was in the range from 2 kPa and - depending on the mixture - up to 50 kPa. Due to the bandwidth limitation, it was only possible to obtain w_e and ND_L for 2 kPa. For the 5%, 10% and 15% mixtures, k_{eff} is pressure-independent, whereas in the case of the 50% mixture, k_{eff} decreases with increasing pressure. For the 20% mixture, the pressure dependence of k_{eff} cannot be observed clearly. w_e in pure R1225ye(Z) is lower than in pure N_2. For R1225ye(Z)/N_2 mixtures, two regions can be distinguished. For E/N values approximately below 120 Td, w_e in mixtures is higher than in pure N_2. Above approximately 120 Td, w_e in mixtures is lower than in pure N_2, and decreases with increasing R1225ye(Z) fraction. The ND_L values for mixtures are lower than for the pure N_2 and decrease with an increasing R1225ye(Z) fraction.

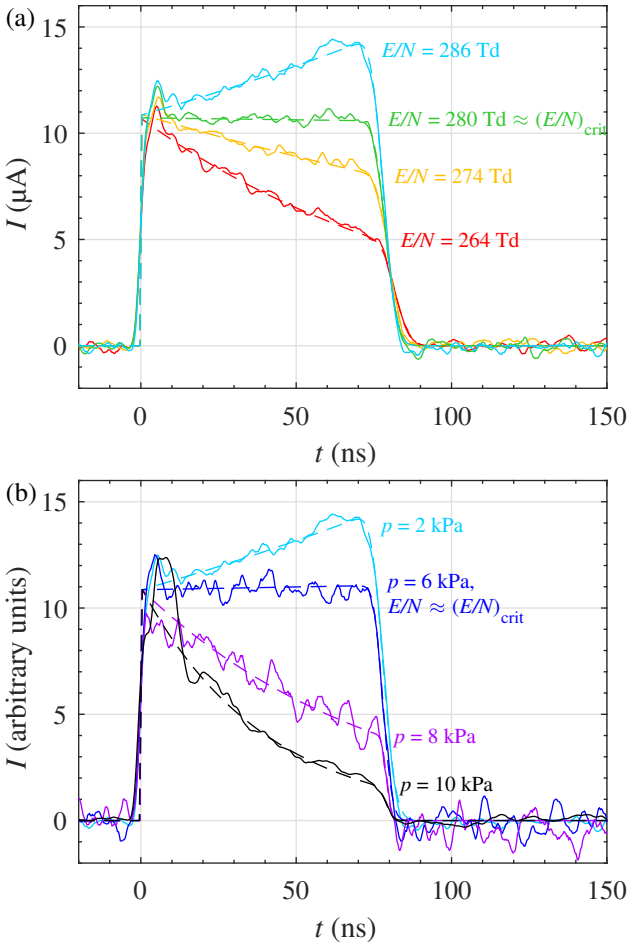

Figure 2. Example electron displacement currents in R1225ye(Z) for an electrode spacing of 13 mm. Solid lines are the extracted electron currents. Dashed lines corresponds to the model of electron current according to equation (1). (a) Fixed pressure of 2 kPa and different E/N values. (b) Fixed E/N value of around 286 Td and different pressure values. The measurements are rescaled to the same initial amplitude for easier comparison.

3.3. R1225ye(Z)/CO_2 mixtures

Figure 4 shows k_{eff}, w_e, and ND_L as functions of E/N for R1225ye(Z)/CO_2 mixtures, with a R1225ye(Z) mole fraction from 5% to 50%. The pressure was in the range from 2 kPa and - depending on the mixture - up to 10 kPa. For all mixtures, k_{eff} appears to remain pressure-independent for the investigated pressure range. w_e in mixtures from 5% to 20% is similar to pure CO_2, while in the 50% mixture, w_e seems to be in between CO_2 and pure R1225ye(Z). The ND_L values of mixtures are below the values of pure CO_2 and decrease with increasing R1225ye(Z) percentage.

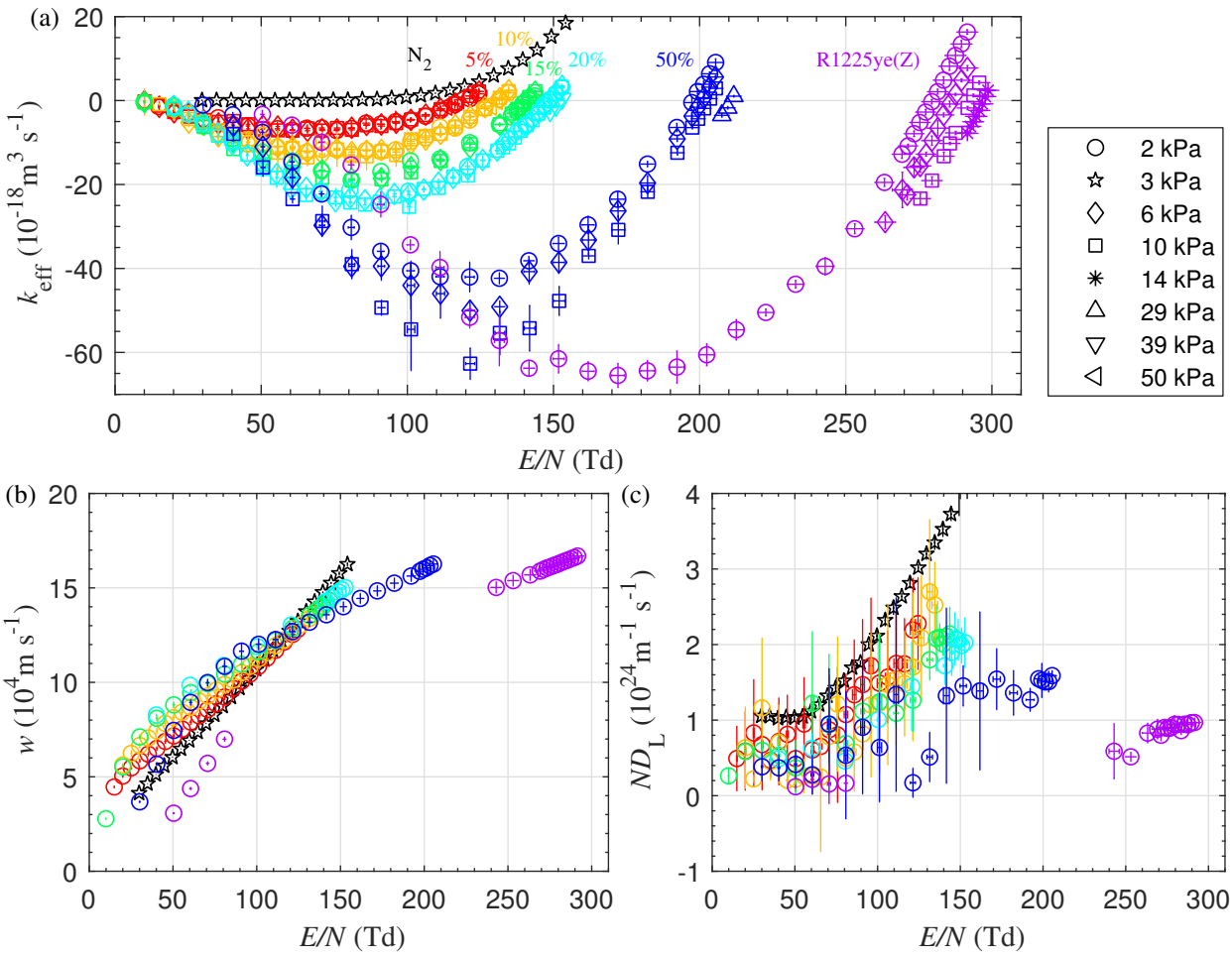

Figure 3. (a) Effective ionization rate coefficient, (b) electron drift velocity, (c) density normalized longitudinal electron diffusion coefficient versus E/N in R1225ye(Z), N_2 [18], and their mixtures. The gas mixtures are color-coded. The gas pressures are indicated by different markers. The percentages of R1225ye(Z) and pressures are indicated in figure (a), the same color and marker code is used for figures (b) and (c).

4. Discussion

4.1. Comparison of R1225ye(Z) with HFO1234ze(E) and 1−C_3F_6

$(E/N)_{crit}$ of pure R1225ye(Z) increases with increasing gas pressure. This pressure dependence has been observed previously for gases with similar structures, namely 1-C_3F_6 [5] and HFO1234ze(E) [3]. As illustrated in figure 5, these three gases have the same C-C=C backbone structure and the same number of member elements, which are fluorine (F) and hydrogen (H). While 1-C_3F_6 has no H-atoms, HFO1234ze(E) has two H-atoms, and R1225ye(Z) with one H-atom is structurally in-between.

The comparison of $(E/N)_{crit}$ of these three gases is shown in figure 6. R1225ye(Z) has the highest critical field in the pressure range from 2 kPa to 14 kPa. For higher pressures, $(E/N)_{crit}$ cannot be reliably predicted, as explained in detail in the next subsection. However, as a rough estimation, upper and lower limits of $(E/N)_{crit}$ can be given. A linear extrapolation gives the upper limit of $(E/N)_{crit} \simeq 350$ Td at a pressure of 50 kPa, and $(E/N)_{crit} \simeq 415$ Td at 94 kPa. Here, 94 kPa is the maximum possible pressure of pure R1225ye(Z) that can be achieved without liquefaction down to 248 K by filling at 293 K. The lower limit is derived under the assumption of an immediate saturation of the pressure dependence and consequently an $(E/N)_{crit}$ of 300 Td. In the case of the upper limit, $(E/N)_{crit}$ of R1225ye(Z) would be superior to 1-C_3F_6 and HFO1234ze(E). In the case of the lower limit, $(E/N)_{crit}$ of R1225ye(Z) would be beneath 1-C_3F_6, but still superior to HFO1234ze(E) up to a pressure of at least 45 kPa.

As mentioned above, an important aspect of the insulation performance under operating conditions is the boiling point - which limits the possible maximum pressure of the gas. The vapor pressure curve of

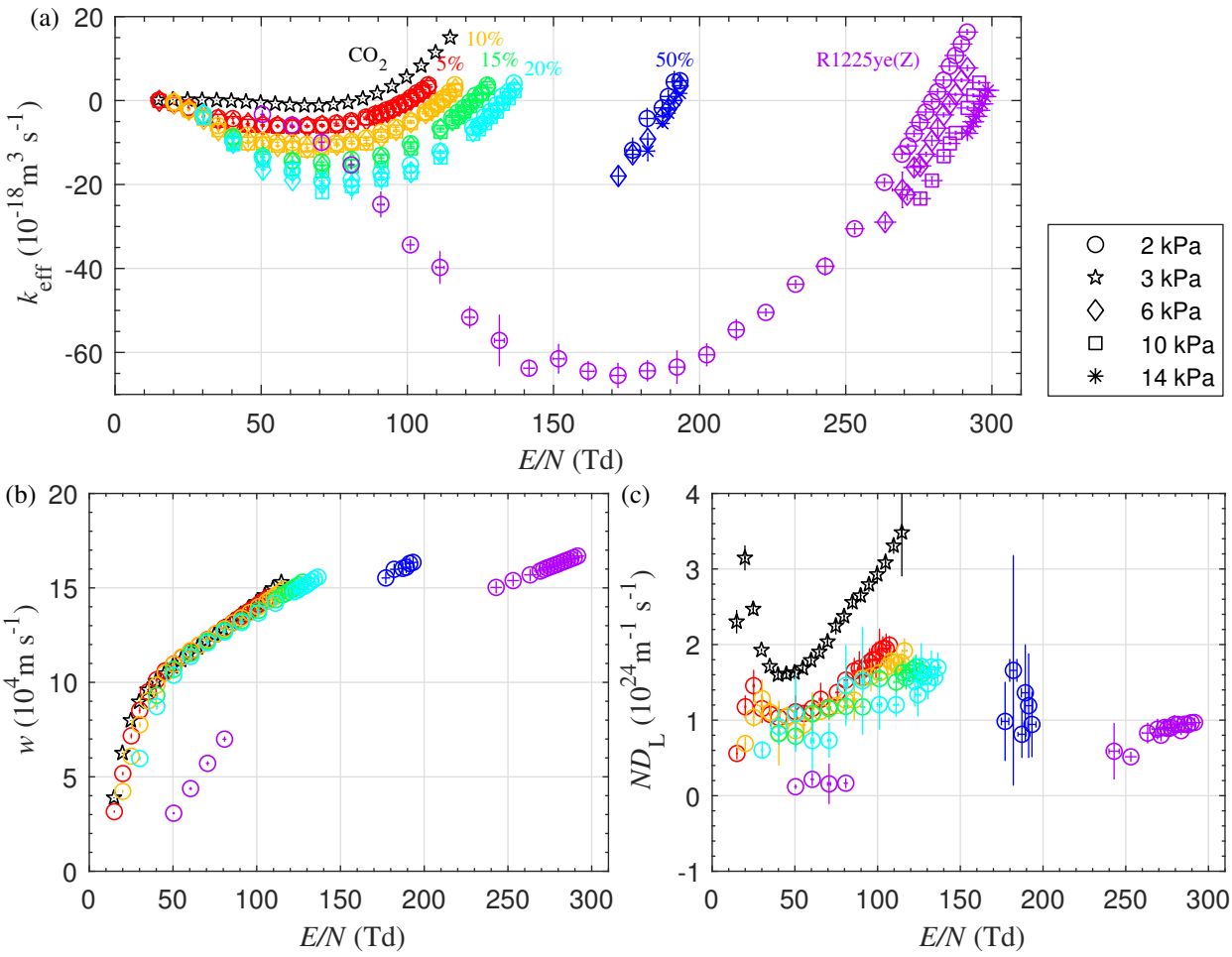

Figure 4. (a) Effective ionization rate coefficient, (b) electron drift velocity, (c) density normalized longitudinal electron diffusion coefficient versus E/N in R1225ye(Z), CO_2 [18], and their mixtures. The gas mixtures are color-coded. The gas pressures are indicated by different markers. The percentages of R1225ye(Z) and pressures are indicated in figure (a), the same color and marker code is used for figures (b) and (c).

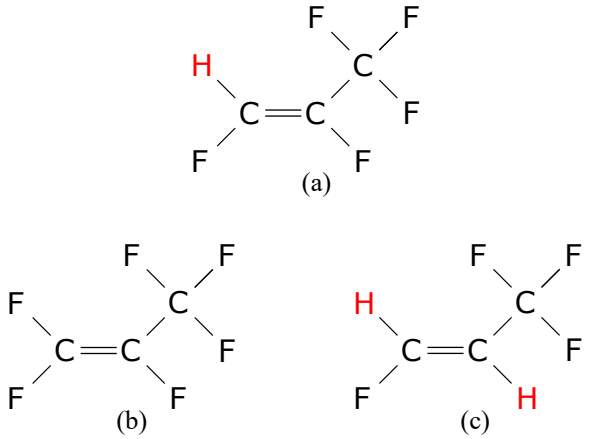

Figure 5. Molecular structure of (a) R1225ye(Z)/C_3HF_5, CAS 5528-43-8, (b) 1-C_3F_6, CAS 116-15-4, (c) HFO1234ze(E)/$C_3H_2F_4$, CAS 1645-83-6.

R1225ye(Z), HFO1234ze(E), and 1-C_3F_6 are shown in figure 7. The vapor pressure curve of R1225ye(Z), with a normal boiling point of approximately 253 K, is almost equal to the vapor pressure curve of HFO1234ze(E), irrespective of the different number of H-atoms. Regarding the combination of $(E/N)_{\mathrm{crit}}$ and boiling point, 1-C_3F_6 has the best insulation performance of these three gases. However, 1-C_3F_6 is supposed to have a high toxicity, with a LC_{50} for 4 h inhalation by rats below 3 000 ppm [19]. Due to the similar boiling point, the superiority of R1225ye(Z) to HFO1234ze(E) depends on $(E/N)_{\mathrm{crit}}$ and is given up to a pressure of at least 45 kPa.

4.2. Three-body electron attachment to R1225ye(Z)

The pressure dependence of $(E/N)_{\mathrm{crit}}$ can be explained with the mechanism of three-body electron attachment [3, 22, 23]. This mechanism can be modeled with processes and corresponding rates of dissociative attach-

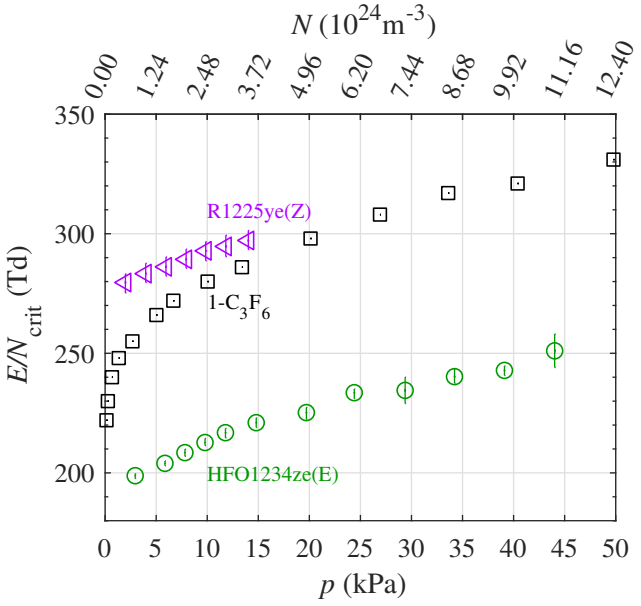

Figure 6. $(E/N)_{\mathrm{crit}}$ of R1225ye(Z), HFO1234ze(E) [3] and 1-C_3F_6 [5] as a function of pressure at 293 K and molecule number density.

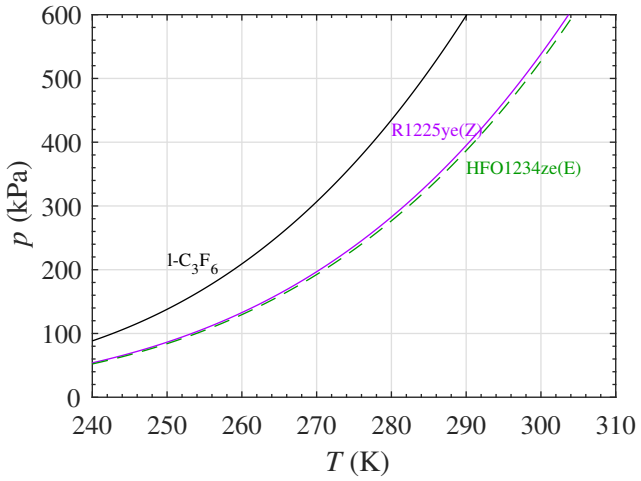

Figure 7. Vapor pressure curves of R1225ye(Z) [8], HFO1234ze(E) [20] and 1-C_3F_6 [21].

ment (k_{da}, equation (2)), parent ion attachment, and autodetachment (k_{at}, τ^{-1}, equation (3)), collisional stabilization (k_{stab}, equation (4)), and collisional detachment (k_{det}, equation (5)) [3].

$$C_3HF_5 + e \xrightarrow{k_{\mathrm{da}}} A^- + B, \tag{2}$$

$$C_3HF_5 + e \underset{\tau^{-1}}{\overset{k_{\mathrm{at}}}{\rightleftharpoons}} (C_3HF_5)^*, \tag{3}$$

$$(C_3HF_5)^* + C_3HF_5 \xrightarrow{k_{\mathrm{stab}}} {C_3HF_5}^- + C_3HF_5, \tag{4}$$

$$(C_3HF_5)^* + C_3HF_5 \xrightarrow{k_{\mathrm{det}}} e + C_3HF_5 + C_3HF_5, \tag{5}$$

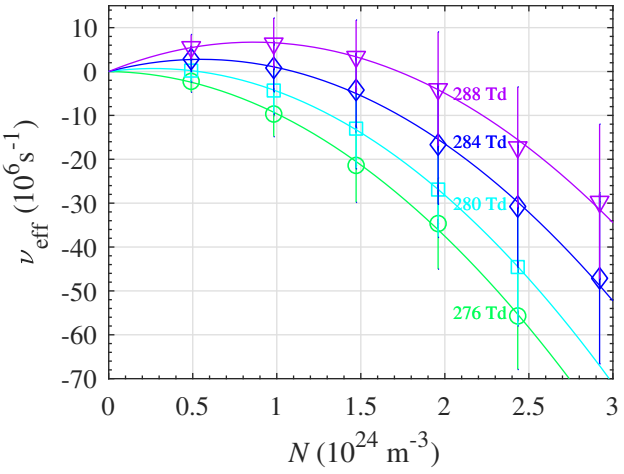

Figure 8. Regression of ν_{eff} for sample E/N values with equation (7).

After several autodetachment lifetimes τ, the effective ionization rate ν_{eff} can be expressed as

$$\nu_{\mathrm{eff}}(N) = (k_{\mathrm{i}} - k_{\mathrm{da}})N - \frac{k_{\mathrm{quad}}N^2}{1 + N/N_{sat}} \tag{6}$$

with the two-body rate coefficient $(k_{\mathrm{i}} - k_{\mathrm{da}})$ consisting of the difference of the total ionization rate coefficient and the dissociative attachment rate coefficient, the saturation density for three-body attachment $N_{\mathrm{sat}} = ((k_{\mathrm{stab}} + k_{\mathrm{det}}) \cdot \tau)^{-1}$, and the three-body attachment rate coefficient $k_{\mathrm{quad}} = k_{\mathrm{at}} \cdot k_{\mathrm{stab}} \cdot \tau$. Two limiting cases can be distinguished, which simplify the equation (6) either to

$$\nu_{\mathrm{eff}}(N) = (k_{\mathrm{i}} - k_{\mathrm{da}})N - k_{\mathrm{quad}}N^2, \tag{7}$$

or to

$$\nu_{\mathrm{eff}}(N) = (k_{\mathrm{i}} - k_{\mathrm{da}})N - k_{\mathrm{quad}}N_{\mathrm{sat}}N. \tag{8}$$

For $N \ll N_{\mathrm{sat}}$ equation (7) is valid. ν_{eff} has a quadratic dependence on N. In this case, a pressure dependence of $(E/N)_{\mathrm{crit}}$ is visible. For $N \gg N_{sat}$ the equation (8) is valid. ν_{eff} grows linearly with N. In this case, no pressure dependence of $(E/N)_{\mathrm{crit}}$ is visible [3].
Figure 8 shows that ν_{eff} of R1225ye(Z) fits to equation (7). Consequently, the investigated pressure range of R1225ye(Z) up to 14 kPa corresponds to the case $N \ll N_{\mathrm{sat}}$. For this case, it is not possible to determine N_{sat}, as it does not appear in equation (7). With the unknown value of N_{sat}, it is not possible to predict $(E/N)_{\mathrm{crit}}$ for pressures higher than what were measured, since the three-body attachment could reach the saturation at a certain gas density. In this case, equation (8) becomes valid, and ν_{eff}/N becomes pressure-independent.

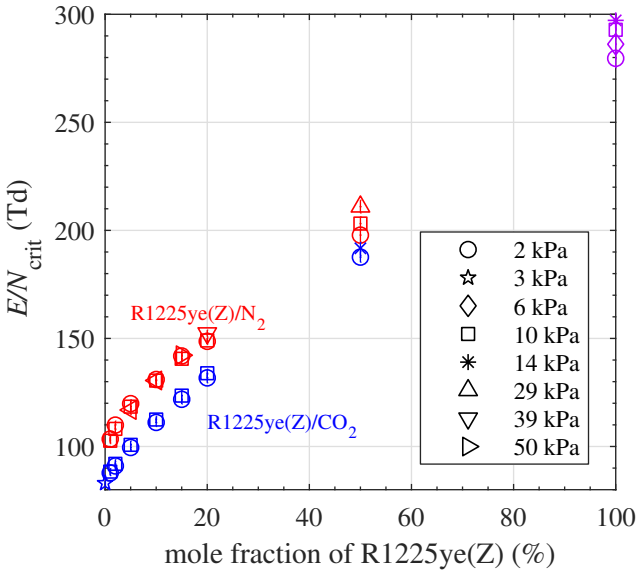

Figure 9. $(E/N)_{crit}$ of R1225ye(Z) mixtures with N_2 (red) and CO_2 (blue).

4.3. Mixtures with buffer gases N_2 and CO_2

R1225ye(Z) shows almost no synergy with N_2 and CO_2. The density reduced critical electric fields $(E/N)_{crit}$ of R1225ye(Z) mixtures with N_2 and CO_2 at different pressures are summarized in figure 9. The results can be split into two regions. In the region up to 15%, the curves exhibit a bowing effect, and no pressure dependence is visible in the investigated range up to 50 kPa with N_2, and up to 10 kPa with CO_2. In the region above 15%, $(E/N)_{crit}$ increases linearly with an increasing R1225ye(Z) fraction, and a pressure dependence is visible.

5. Conclusion

$(E/N)_{crit}$ of R1225ye(Z) is pressure dependent, as was previously observed for gases with similar structures: HFO1225ze(E) and 1-C_3F_6. According to the combination of the $(E/N)_{crit}$ and the boiling point, the insulating performance of pure R1225ye(Z) is superior to HFO1225ze(E), up to a pressure of at least 45 kPa, but inferior to 1-C_3F_6 or SF_6. In the investigated pressure range, R1225ye(Z) shows almost no synergy with N_2 and CO_2. The prediction of $(E/N)_{crit}$ for operating pressures of pure R1225ye(Z) and its mixtures is not possible, due to the possible saturation of the three-body attachment and unknown synergy behavior with buffer gases for higher pressures. Future investigations should be made to investigate the electric strength at higher pressures.
R1225ye(Z) could be considered as an insulation gas for medium voltage applications, due to its higher electric strength than HFO1234ze(E), equally low GWP<1, and the same boiling point.

Acknowledgments

This work is financially supported by GE Grid (Switzerland) GmbH, Pfiffner Technologie AG, ABB Switzerland Ltd and Siemens AG.

References

[1] M Rabie, DA Dahl, SMA Donald, M Reiher and CM Franck. "Predictors for gases of high electrical strength". In: *IEEE Transactions on Dielectrics and Electrical Insulation* 20.3 (June 2013), pp. 856–863. ISSN: 1070-9878. DOI: 10.1109/TDEI.2013.6518955.

[2] M Rabie and CM Franck. "Computational screening of new high voltage insulation gases with low global warming potential". In: *IEEE Transactions on Dielectrics and Electrical Insulation* 22.1 (Feb. 2015), pp. 296–302. ISSN: 1070-9878. DOI: 10.1109/TDEI.2014.004474.

[3] A Chachereau, M Rabie, and CM Franck. "Electron swarm parameters of the hydrofluoroolefine HFO1234ze". In: *Plasma Sources Science and Technology* 25.4 (2016), p. 045005. URL: http://stacks.iop.org/0963-0252/25/i=4/a=045005.

[4] A Chachereau and CM Franck. "Characterization of HFO1234ze mixtures with N2 and CO2 for use as gaseous electrical insulation media". In: *Proceedings of the 20th International Symposium on High Voltage Engineering (ISH 2017)*. Cigre. 2017.

[5] T Aschwanden. "Die Ermittlung physikalischer Entladungsparameter in Isoliergasen und Isoliergasgemischen mit einer verbesserten Swarm-Methode". PhD thesis. ETH Zurich, 1985. URL: http://e-collection.library.ethz.ch/view/eth:36996.

[6] G Myhre, D Shindell, F-M Breon, W Collins, J Fuglestvedt, J Huang, D Koch, J-F Lamarque, D Lee, B Mendoza, T Nakajima, A Robock, G Stephens, T Takemura and H Zhang. "Anthropogenic and Natural Radiative Forcing". In: *Climate Change 2013: The Physical Science Basis. Contribution of Working Group I to the Fifth Assessment Report of the Intergovernmental Panel on Climate Change*. Ed. by TF Stocker et al. Cambridge, United Kingdom and New York, NY, USA: Cambridge University Press, 2013. Chap. 8, pp. 659–740. ISBN: 978-1-107-66182-0. DOI: 10.1017/CBO9781107415324.018. URL: www.climatechange2013.org.

[7] AA Lindley and TJ Noakes. "Consideration of Hydrofluoroolefins (HFOs) as potential candidate medical propellants". In: *Mexichem Fluor online publication, (www.mexichemfluor.com)* (2010).

[8] L Fedele, G Di Nicola, JS Brown, L Colla and S Bobbo. "Saturated pressure measurements of cis-pentafluoroprop-1-ene (R1225ye (Z))". In: *International Journal of Refrigeration* 69 (2016), pp. 243–250. DOI: https://doi.org/10.1016/j.ijrefrig.2015.10.012. URL: http://www.sciencedirect.com/science/article/pii/S0140700715003072.

[9] Apollo Scientific Ltd. *Safety data sheet (Z)-1,2,3,3,3-PENTAFLUOROPROPENE*. 2016.

[10] Synquest Laboratories. *(Z)-1,2,3,3,3-Pentafluoropropene Safety Data Sheet 13003Z5*. 2015.

[11] PJ Chantry and RE Wootton. "A critique of methods for calculating the dielectric strength of gas mixtures". In: *Journal of Applied Physics* 52.4 (1981), pp. 2731–2739. ISSN: 00218979. DOI: 10.1063/1.329081. URL: http://scitation.aip.org/content/aip/journal/jap/52/4/10.1063/1.329081.

[12] SR Hunter and LG Christophorou. "Pressure-dependent electron attachment and breakdown strengths of unary gases and synergism of binary gas mixtures: A relationship". In: *Journal of Applied Physics* 57.9 (1985), pp. 4377–4385. DOI: 10.1063/1.334598. URL: https://doi.org/10.1063/1.334598.

[13] Apollo Scientific Ltd. *Certificate of analysis for a typical batch*. 2016.

[14] International Electrotechnical Commission. "IEC 62271-1: 2007. High-voltage switchgear and controlgear-Part 1: Common specifications". In: *International Electrotechnical Commission* (2007), p. 252.

[15] DA Dahl, TH Teich, and CM Franck. "Obtaining precise electron swarm parameters from a pulsed Townsend setup". In: *Journal of Physics D: Applied Physics* 45.48 (2012), p. 485201. URL: http://stacks.iop.org/0022-3727/45/i=48/a=485201.

[16] *LXcat Plasma Data Exchange Project*. URL: www.lxcat.net.

[17] LC Pitchford, LL Alves, K Bartschat, SF Biagi, M-C Bordage, I Bray, CE Brion, MJ Brunger, L Campbell, A Chachereau and others. "LXCat: an Open-Access, Web-Based Platform for Data Needed for Modeling Low Temperature Plasmas". In: *Plasma Processes and Polymers* 14.1-2 (2017), p. 1600098.

[18] P Haefliger and CM Franck. "Detailed precision and accuracy analysis of swarm parameters from a pulsed Townsend experiment". In: *Review of Scientific Instruments* 89.2 (2018), p. 023114.

[19] GL Kennedy. "Toxicology of Fluorine-Containing Monomers". In: *Critical reviews in toxicology* 21.2 (1990), pp. 149–170. DOI: 10.3109/10408449009089877. URL: https://doi.org/10.3109/10408449009089877.

[20] G Di Nicola, JS Brown, L Fedele, S Bobbo and C Zilio. "Saturated pressure measurements of trans-1, 3, 3, 3-tetrafluoroprop-1-ene (R1234ze (E)) for reduced temperatures ranging from 0.58 to 0.92". In: *Journal of Chemical & Engineering Data* 57.8 (2012), pp. 2197–2202.

[21] GH Whipple. "Vapor-liquid equilibria of some fluorinated hydrocarbon systems". In: *Industrial & Engineering Chemistry* 44.7 (1952), pp. 1664–1667.

[22] LG Christophorou and SR Hunter. *Electrons in dense gases Swarms of Ions and Electrons in Gases ed W Lindinger et al.* 1984.

[23] NL Aleksandrov. "Three-body electron attachment to a molecule". In: *Soviet Physics Uspekhi* 31.2 (1988), p. 101. URL: http://stacks.iop.org/0038-5670/31/i=2/a=R01.